Scientific Research Publishing

Open Journal of Applied Sciences, 2026, 16(11), 4703-4713
https://www.scirp.org/journal/ojapps
ISSN Online: 2165-3925
ISSN Print: 2165-3917

Effects of Image Perturbations on the Accuracy of Full-Field Displacement Measurements Using 3D Digital Image Correlation

Pengming Xie[1], Menglian Liu[1,2], Cui Fang[3], Lin Dai[3], Xian Wang[1,4]

[1]School of Mechanical Engineering, Hunan University of Science and Technology, Xiangtan, China
[2]Nanyue Fuel Injection Systems Co., Ltd., Hengyang, China
[3]Hunan Institute of Metrology and Test, Changsha, China
[4]State Key Laboratory of Offshore Wind Power Equipment and Wind Energy High-Efficient Utilization, Xiangtan, China
Email: 15773923218@163.com

How to cite this paper: Xie, P.M., Liu, M.L., Fang, C., Dai, L. and Wang, X. (2026) Effects of Image Perturbations on the Accuracy of Full-Field Displacement Measurements Using 3D Digital Image Correlation. *Open Journal of Applied Sciences*, **16**, 4703-4713.
https://doi.org/10.4236/ojapps.2026.1611259

Received: October 14, 2026
Accepted: November 22, 2026
Published: November 25, 2026

Copyright © 2026 by author(s) and Scientific Research Publishing Inc.
This work is licensed under the Creative Commons Attribution International License (CC BY 4.0).
http://creativecommons.org/licenses/by/4.0/

Open Access

Abstract

Three-dimensional digital image correlation (3D-DIC) can achieve subpixel accuracy under laboratory conditions, but camera motion in field applications can reduce measurement accuracy. This study investigates the effects of prescribed two-dimensional image translations, in-plane rotations, and their combination on three-dimensional displacement measurements obtained using a calibrated stereo-DIC system. Without camera perturbations, the root mean square errors (RMSEs) in the X-, Y-, and Z-directions were 0.012, 0.014, and 0.007 mm, respectively. Horizontal image translation primarily affected the X-direction measurements, with the mean absolute error (MAE) reaching 0.2664 mm at a translation of 1.5 pixels. Rotational perturbations introduced spatially nonuniform, banded errors. At a rotation of 1.5˚, the Y-direction RMSE reached 1.1217 mm. Combined translation and rotation produced a larger Y-direction error than the corresponding individual perturbations. These results characterize displacement measurement errors under the prescribed image perturbations and provide a basis for subsequent camera-motion compensation studies.

Keywords

Optical Measurement, Three-Dimensional Digital Image Correlation, Image Perturbations, Displacement Measurement

1. Introduction

Structural displacement is an important indicator of a structure's response to

loading and deformation. Accurate displacement measurements support structural condition assessment and safety monitoring [1] [2]. Digital image correlation (DIC) measures surface displacements without physical contact by matching grayscale patterns in images acquired before and after deformation [3]. Three-dimensional digital image correlation (3D-DIC) combines image correlation with stereo vision to reconstruct surface coordinates at different times and determine full-field three-dimensional displacements [4].

In conventional 3D-DIC measurements with fixed calibration parameters, camera motion alters the imaging geometry and introduces apparent displacements into the results. In field applications, wind and ground vibrations can cause camera translation or rotation, reducing measurement accuracy. For a stereo system, rigid-body motion of the camera pair changes the relationship between the measurement coordinate system and the structure, whereas relative motion between the cameras also changes the relative extrinsic parameters of the stereo system. These two types of motion affect displacement measurements differently and therefore require distinct treatment in error analysis [5].

Camera-motion-induced errors have been investigated in both monocular and stereo DIC. For monocular DIC, Li [6] decomposed camera motion into three translational and three rotational components and analyzed the resulting image deformation and displacement errors. Selected motion conditions were examined through simulations and physical experiments. For stereo DIC, Shao and He [5] used controlled speckle-pattern simulations to investigate systematic errors caused by rigid-body motion of the camera pair and relative motion between the cameras. They also proposed a speckle-based method to compensate for errors caused by relative camera motion.

Existing compensation methods use different approaches to estimate camera motion. Lee *et al*. [7] used a main camera to measure target displacement and a rigidly attached auxiliary camera to estimate camera ego-motion, reducing motion-induced errors in long-term displacement measurements. Xing *et al*. [8] developed a dual-view system comprising a camera, a beam splitter, a convex lens, and a photomask to compensate for both camera motion and thermal effects on the image sensor. X. Liu *et al*. [9] constructed a network of rigidly connected measurement and calibration cameras and estimated observation-platform motion using reference control points. M. Liu *et al*. [10] combined automatic reference-feature selection with depth constraints to improve camera ego-motion compensation in complex scenes. These methods provide different approaches to identifying and correcting camera-motion-induced errors, with their implementation depending on the optical configuration and available reference information.

This study examines errors in the three displacement components of a calibrated stereo-DIC system under prescribed two-dimensional image perturbations. Image translations, in-plane rotations, and their combinations are applied to acquired images, and displacement fields are calculated using the same correlation parameters across the tested conditions. The resulting errors are evaluated

using mean absolute error and root mean square error. The imposed transformations are defined in image coordinates and do not constitute complete simulations of physical camera motion. In particular, this study does not separately model rigid-body motion of the stereo camera pair and relative motion between the cameras. The findings are therefore restricted to the prescribed image perturbations and the stereo configuration examined here.

2. Principles of 3D-DIC Displacement Measurement

3D-DIC combines image correlation with stereo vision to reconstruct the three-dimensional coordinates of a target point from its corresponding positions in the left and right images. Displacement is then determined from changes in these coordinates over time [4]. The measurement procedure in this study consists of camera calibration, image correlation, three-dimensional reconstruction, and displacement calculation. This section presents the basic relationships underlying these steps. These relationships provide the basis for the subsequent analysis of measurement errors under translational, rotational, and combined image transformations.

2.1. Camera Imaging Model

Camera imaging is described by the pinhole model. A spatial point is first transformed from the world coordinate system to the camera coordinate system using the extrinsic parameters and then projected onto the image plane using the intrinsic parameters. The camera intrinsic parameters can be estimated using Zhang's planar calibration method [11]. Let $\boldsymbol{P}_w = \left[X_w, Y_w, Z_w\right]^{\mathrm{T}}$ and $\boldsymbol{P}_c = \left[X_c, Y_c, Z_c\right]^{\mathrm{T}}$ denote the coordinates of a spatial point in the world and camera coordinate systems, respectively. Their relationship is given by

$$\begin{bmatrix} X_c \\ Y_c \\ Z_c \end{bmatrix} = \boldsymbol{R} \begin{bmatrix} X_w \\ Y_w \\ Z_w \end{bmatrix} + \boldsymbol{T} \tag{1}$$

where $\boldsymbol{R}$ is a 3×3 rotation matrix and $\boldsymbol{T}$ is a 3×1 translation vector. Together, they describe the transformation from the world coordinate system to the camera coordinate system. Let (x, y) denote the ideal pixel coordinates of the spatial point. From similar triangles, the projection from camera coordinates to pixel coordinates is expressed as

$$s\begin{bmatrix} x \\ y \\ 1 \end{bmatrix} = \boldsymbol{K} \begin{bmatrix} X_c \\ Y_c \\ Z_c \end{bmatrix} \tag{2}$$

where s is the projective scale factor and $\boldsymbol{K}$ is the camera intrinsic matrix, which contains parameters such as the focal lengths in pixel units and the principal point coordinates. Equation (2) describes ideal pinhole projection; lens distortion must be treated separately.

In practice, lens distortion causes image coordinates to deviate from their ideal

projected positions. Both radial and tangential distortion generally need to be considered. Tangential distortion is associated with factors such as lens decentering [12]. Before three-dimensional reconstruction, the image coordinates of matched points should therefore be corrected using the calibrated distortion parameters. The pixel coordinates used in the stereo reconstruction equations below are corrected for lens distortion.

2.2. Image Matching and Three-Dimensional Reconstruction

Digital image correlation identifies the corresponding position of each reference-image subset in the target image. In this study, the zero-mean normalized sum of squared differences (ZNSSD) is used as the correlation criterion [13]:

$$C_{\mathrm{ZNSSD}} = \sum_{i=1}^{N} \left[\frac{f_i - \overline{f}}{\sqrt{\sum_{j=1}^{N} \left(f_j - \overline{f} \right)^2}} - \frac{g_i - \overline{g}}{\sqrt{\sum_{j=1}^{N} \left(g_j - \overline{g} \right)^2}} \right]^2 \tag{3}$$

where f_i and g_i are the grayscale intensities at the i th sampling point in the reference subset and its corresponding location in the target image, respectively. The quantities $\overline{f}$ and $\overline{g}$ are the mean grayscale intensities of the two subsets, and N is the number of sampling points in a subset. A value of C_{ZNSSD} closer to zero indicates a better match. Subpixel displacement estimation was performed using the inverse compositional Gauss-Newton (IC-GN) algorithm. Starting from an initial displacement estimate, the shape-function parameters were iteratively refined to minimize the ZNSSD criterion. A subset size of 31×31 pixels and a first-order shape function are used throughout the subsequent experiments. The mapping between the reference and target subsets is expressed as

$$\begin{cases} x' = x + u_0 + u_x \Delta x + u_y \Delta y, \\ y' = y + v_0 + v_x \Delta x + v_y \Delta y \end{cases} \tag{4}$$

where (x, y) and (x', y') denote the pixel coordinates in the reference and target images, respectively. The local coordinates $\Delta x = x - x_0$ and $\Delta y = y - y_0$ represent the offsets from the reference subset center (x_0, y_0). The quantities u_0 and v_0 are the displacement components at the subset center, while u_x, u_y, v_x, and v_y are the first-order spatial derivatives of the displacement components evaluated at that center.

The initial speckle image acquired by the left camera is used as the reference image. Stereo matching is first performed between synchronized left and right images to establish correspondence between subsets at the same instant. Temporal matching is then performed to track the corresponding subsets over time. The processing procedure is shown in **Figure 1**.

For three-dimensional reconstruction, let (x_L, y_L) and (x_R, y_R) denote the distortion-corrected coordinates of corresponding subset centers in the left and right images acquired at the same instant. Using the calibrated camera parameters, the projection relationships are written as

$$\begin{cases} s_L \begin{bmatrix} x_L \\ y_L \\ 1 \end{bmatrix} = \boldsymbol{M}_L \begin{bmatrix} X_w \\ Y_w \\ Z_w \\ 1 \end{bmatrix}, \\ s_R \begin{bmatrix} x_R \\ y_R \\ 1 \end{bmatrix} = \boldsymbol{M}_R \begin{bmatrix} X_w \\ Y_w \\ Z_w \\ 1 \end{bmatrix} \end{cases} \tag{5}$$

where $\boldsymbol{M}_L$ and $\boldsymbol{M}_R$ are the 3×4 projection matrices of the left and right cameras, respectively, and s_L and s_R are the corresponding projective scale factors. After eliminating the scale factors, the three-dimensional coordinates (X_w, Y_w, Z_w) can be determined by solving the resulting linear system in the least-squares sense. Displacement is then calculated as the difference between the reconstructed coordinates of the same point at the current and reference times.

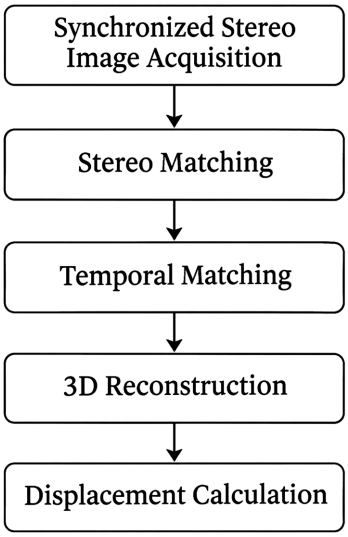

Figure 1. Processing workflow for 3D-DIC.

3. Image Perturbation Experiments

The stereo vision system consisted of two Point Grey industrial cameras, each with an image resolution of 2048 × 2048 pixels and a lens with a nominal focal length of 12 mm. Sixteen stereo image pairs of a checkerboard were acquired at different orientations for calibration. Camera calibration was performed using Zhang's method with the camera calibration toolbox in MATLAB R2022a. The mean reprojection errors of the left and right cameras were 0.0734 and 0.0669 pixels, respectively, giving an overall mean of approximately 0.07 pixels. The intrinsic calibration parameters are summarized in Table 1. After calibration, the baseline displacement measurement performance was evaluated using a three-axis translation stage. The speckle target was moved in ten steps of 0.1 mm along each of the X-, Y-, and Z-directions. The measured displacements were compared with

the nominal stage displacements, yielding RMSEs of 0.012, 0.014, and 0.007 mm, respectively. These results characterize the baseline measurement performance without imposed image perturbations.

Table 1. Intrinsic calibration parameters of the stereo cameras.

Parameter	Left camera	Right camera
Focal lengths $\left(f_x, f_y\right)$ (pixels)	(2219.38, 2218.44)	(2215.68, 2214.06)
Principal point $\left(u_0, v_0\right)$ (pixels)	(1028.45, 1035.25)	(1029.76, 1024.98)
Skew	0.00	0.00
Radial distortion coefficients $\left(k_1, k_2\right)$	(−0.1243, 0.0793)	(−0.1284, 0.0720)
Mean reprojection error (pixels)	0.0734	0.0669

The displacement measurement errors were evaluated using the root mean square error (RMSE) and mean absolute error (MAE), defined as follows:

$$\mathrm{RMSE} = \sqrt{\frac{1}{N}\sum_{i=1}^{N}\left(D_i - D_i^*\right)^2} \tag{6}$$

$$\mathrm{MAE} = \frac{1}{N}\sum_{i=1}^{N}\left|D_i - D_i^*\right| \tag{7}$$

Here, D_i denotes the measured displacement, D_i^* denotes the true displacement, and N denotes the number of images in the evaluated sequence. Both metrics are expressed in millimeters.

To evaluate the effects of prescribed image perturbations on stereo-DIC displacement measurements, two-dimensional translations, in-plane rotations, and their combinations were applied to the acquired images. These transformations were used to examine the response of the measurement procedure to image perturbations, rather than to reproduce specific physical camera trajectories.

For the translation simulations, image shifts of 0.5 and 1.5 pixels were applied. A region of interest measuring 450 × 450 pixels was selected at the center of the speckle pattern. DIC calculations were performed using a step size of 7 pixels, a subset size of 31 × 31 pixels, and a first-order shape function. **Figure 2** shows the measured displacement fields without imposed image perturbations. **Figure 3** and **Figure 4** show the results under image translations of 0.5 and 1.5 pixels, respectively.

The X-direction MAE increased with the magnitude of the imposed horizontal image translation. At a translation of 0.5 pixels, the X-direction MAE and RMSE were 0.1328 and 0.1329 mm, respectively, compared with 0.0114 and 0.0121 mm without translation. At a translation of 1.5 pixels, the X-direction MAE reached 0.2664 mm. Horizontal image translation primarily affected the X-direction measurement accuracy, with smaller effects on the Y- and Z-direction measurements.

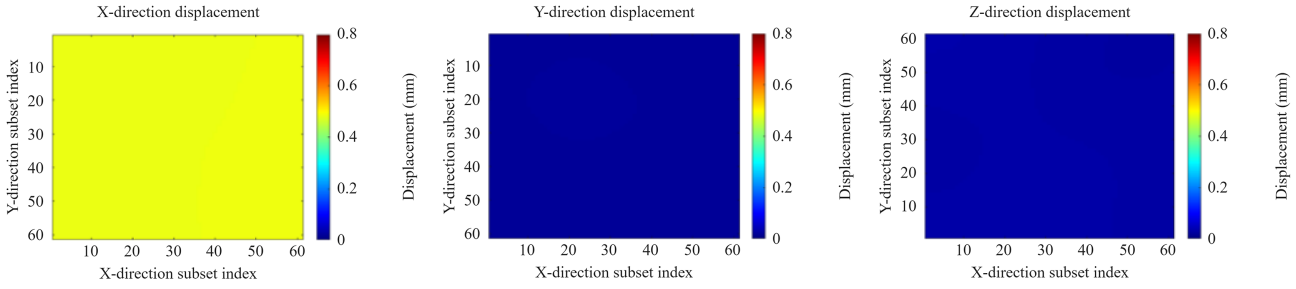

Figure 2. Measured displacement without imposed image perturbations: (a) X-direction displacement; (b) Y-direction displacement; (c) Z-direction displacement.

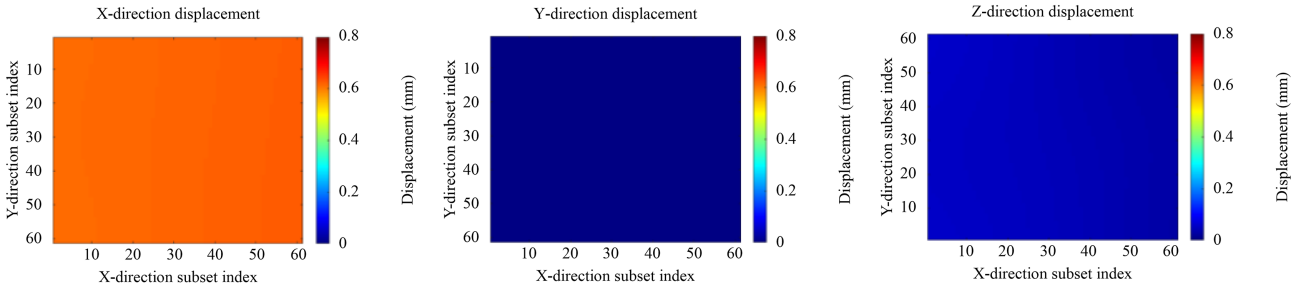

Figure 3. Measured displacement under a 0.5-pixel image translation: (a) X-direction displacement; (b) Y-direction displacement; (c) Z-direction displacement.

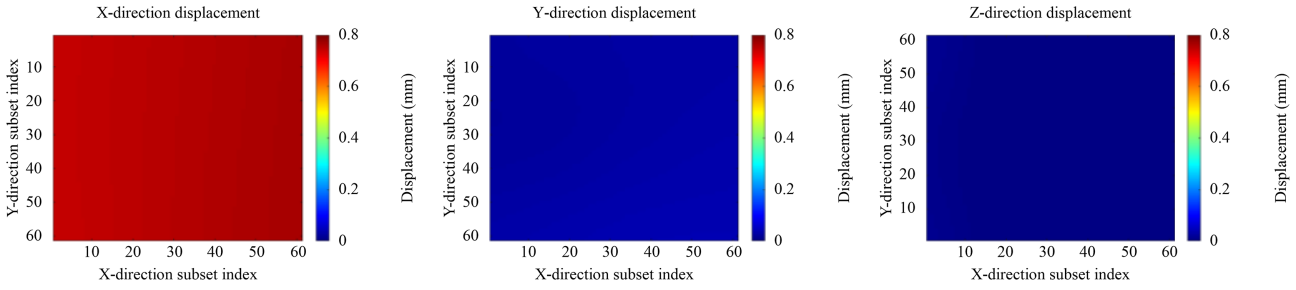

Figure 4. Measured displacement under a 1.5-pixel image translation: (a) X-direction displacement; (b) Y-direction displacement; (c) Z-direction displacement.

For the rotation tests, in-plane image rotations of 0.5˚ and 1.5˚ were applied about the image center. The resulting three-dimensional displacement fields were calculated using 3D-DIC, as shown in Figure 5 and Figure 6.

Rotational perturbations substantially affected the displacement measurements, producing banded displacement patterns. The X-direction RMSE increased from 0.0876 mm at 0.5˚ to 0.2127 mm at 1.5˚. The effect was more pronounced in the Y-direction: the MAE and RMSE were 0.1807 and 0.1976 mm, respectively, at 0.5˚, increasing to 1.0352 and 1.1217 mm at 1.5˚. The increase in the Z-direction errors was comparatively small.

To examine the measurement errors caused by combined rotation and transla-

tion, the images were first rotated by 0.5˚ about the image center and then translated by 0.5 pixels. The measurement results are shown in Figure 7.

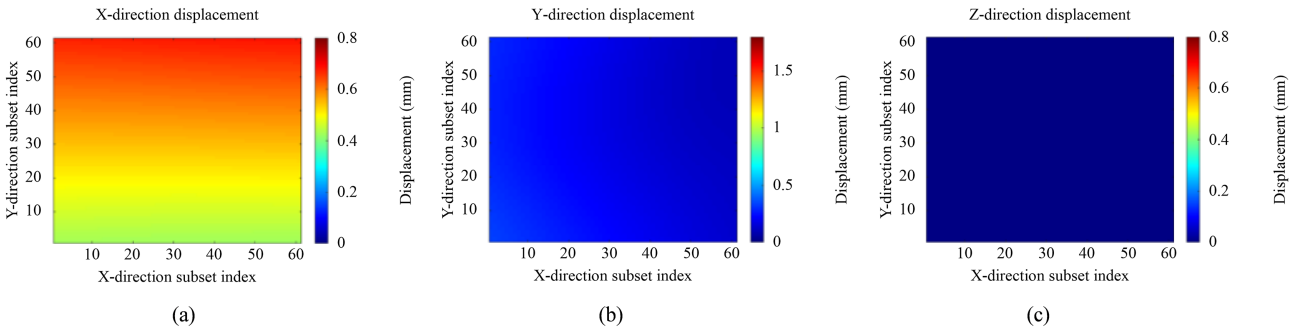

Figure 5. Measured displacement under a 0.5˚ image rotation: (a) X-direction displacement; (b) Y-direction displacement; (c) Z-direction displacement.

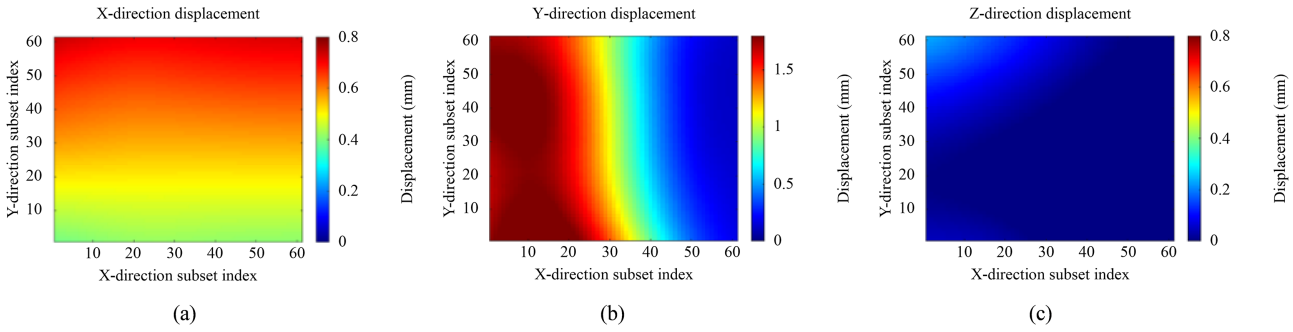

Figure 6. Measured displacement under a 1.5˚ image rotation: (a) X-direction displacement; (b) Y-direction displacement; (c) Z-direction displacement.

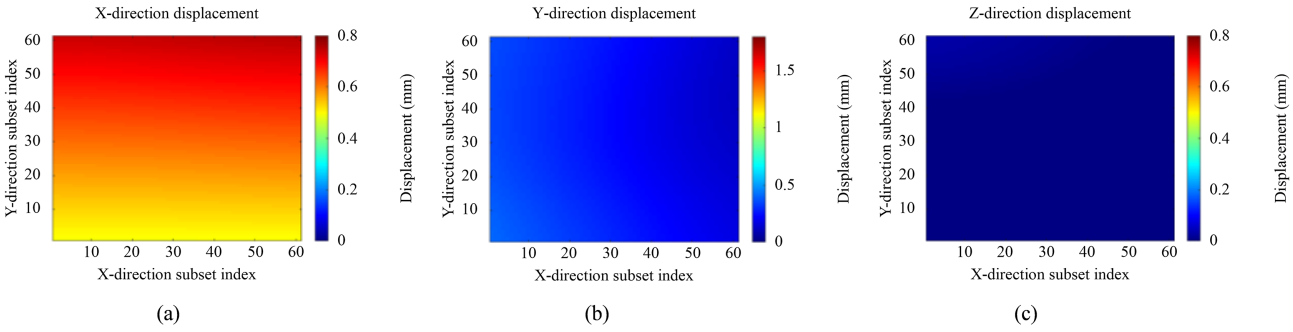

Figure 7. Measured displacement after a 0.5˚ image rotation followed by a 0.5-pixel translation: (a) X-direction displacement; (b) Y-direction displacement; (c) Z-direction displacement.

The X-direction displacement exhibited a banded distribution, with smaller offsets near the central axis and larger offsets toward the sides. The Y-direction displacement showed diagonal bands extending from the upper left to the lower right, with an MAE of 0.2545 mm and an RMSE of 0.2640 mm. The Z-direction displacement varied gradually, with both the MAE and RMSE equal to 0.0165 mm.

The experimental results show that translational motion primarily affects measurement accuracy along the corresponding axis, whereas rotational motion intro-

duces banded errors and has a much greater effect than translation. Combined translation and rotation produce larger measurement deviations than either motion alone. The developed 3D-DIC system can accurately measure small displacements in different directions, with low measurement errors and measured displacement trends that are generally consistent with those of the target displacement.

4. Conclusions

This study evaluated the effects of prescribed two-dimensional image translations, in-plane rotations, and their combination on full-field three-dimensional displacement measurements using a calibrated stereo-DIC system. The main conclusions are as follows:

1) The stereo system achieved a mean reprojection error of 0.07 pixels. Without camera perturbations, the displacement RMSEs in the X-, Y-, and Z-directions were 0.012, 0.014, and 0.007 mm, respectively, providing a baseline for subsequent perturbation analysis.

2) Horizontal translation primarily affected the X-direction measurement accuracy. As the translation increased from 0 to 0.5 and 1.5 pixels, the X-direction MAE increased from 0.0114 mm to 0.1328 and 0.2664 mm, respectively, while changes in the Y- and Z-directions were relatively small. The similar MAE and RMSE values under each translation condition indicate that the error magnitudes were narrowly distributed.

3) Rotational perturbations introduced spatially nonuniform, banded errors. As the image rotation increased from 0.5˚ to 1.5˚, the Y-direction RMSE increased from 0.1976 to 1.1217 mm, while the X-direction RMSE increased from 0.0876 to 0.2127 mm. These observations are limited to the selected perturbation magnitudes and do not establish an intrinsic sensitivity ranking between physical camera translation and rotation.

4) Under combined perturbations, the Y-direction MAE and RMSE were 0.2545 and 0.2640 mm, respectively, both exceeding those under the corresponding individual perturbations. The Z-direction MAE and RMSE were both 0.0165 mm, indicating a comparatively small effect.

The findings are specific to a planar rigid target, fixed calibration parameters, and the prescribed two-dimensional image transformations. They characterize the displacement measurement errors of the tested stereo-DIC configuration under these conditions and do not establish general error relationships for physical six-degree-of-freedom camera motion. Rigid-body motion of the stereo camera pair and relative motion between the cameras require separate investigation using physically consistent imaging models or controlled camera-motion experiments. Future work will combine inertial measurements with stationary reference points to estimate camera pose and evaluate compensation performance under real disturbances.

Acknowledgements

This work was supported by the Natural Science Foundation of Hunan Province

(Grant No. 2024JJ8273) and the Open Research Fund of the State Key Laboratory of Offshore Wind Power Equipment and Wind Energy High-Efficient Utilization (Grant No. HFQZ 2024-14).

Author Contributions

Conceptualization, M.L.L. and P.M.X.; methodology, M.L.L.; validation, P.M.X. and M.L.L.; formal analysis, C.F.; investigation, L.D.; resources, X.W.; data curation, M.L.L.; writing—original draft preparation, P.M.X.; supervision, C.F.; project administration, L.D.; funding acquisition, X.W. All authors have read and agreed to the published version of the manuscript.

Conflicts of Interest

The authors declare no conflicts of interest regarding the publication of this paper.

References

[1] Olaszek, P. (1999) Investigation of the Dynamic Characteristic of Bridge Structures Using a Computer Vision Method. *Measurement*, **25**, 227-236. https://doi.org/10.1016/s0263-2241(99)00006-8

[2] Kim, S., Lee, S., Kim, N. and Kim, D. (2013) Numerical Model Validation for a Prestressed Concrete Girder Bridge by Using Image Signals. *KSCE Journal of Civil Engineering*, **17**, 509-517. https://doi.org/10.1007/s12205-013-0560-1

[3] Peters, W.H. and Ranson, W.F. (1982) Digital Imaging Techniques in Experimental Stress Analysis. *Optical Engineering*, **21**, 427-431.

[4] Chen, F., Chen, X., Xie, X., Feng, X. and Yang, L. (2013) Full-Field 3D Measurement Using Multi-Camera Digital Image Correlation System. *Optics and Lasers in Engineering*, **51**, 1044-1052. https://doi.org/10.1016/j.optlaseng.2013.03.001

[5] Shao, X. and He, X. (2022) Camera Motion-Induced Systematic Errors in Stereo-DIC and Speckle-Based Compensation Method. *Optics and Lasers in Engineering*, **149**, Article 106809. https://doi.org/10.1016/j.optlaseng.2021.106809

[6] Li, F.N. (2024) Analysis and Experimented Verification of Factors Affecting the Accuracy of Deformation Testing via Digital Image Correlation. Master's Thesis, Guangxi University.

[7] Lee, J., Lee, K.C., Jeong, S., Lee, Y.J. and Sim, S.H. (2020) Long-Term Displacement Measurement of Full-Scale Bridges Using Camera Ego-Motion Compensation. *Mechanical Systems and Signal Processing*, **140**, Article 106651. https://doi.org/10.1016/j.ymssp.2020.106651

[8] Xing, L., Dai, W. and Zhang, Y. (2022) Improving Displacement Measurement Accuracy by Compensating for Camera Motion and Thermal Effect on Camera Sensor. *Mechanical Systems and Signal Processing*, **167**, Article 108525. https://doi.org/10.1016/j.ymssp.2021.108525

[9] Liu, X., Hu, B., Yin, Y., Zhang, Y., Chen, W., Yu, Q., *et al.* (2024) Parallel Camera Network: Motion-Compensation Vision Measurement Method and System for Structural Displacement. *Automation in Construction*, **165**, Article 105559. https://doi.org/10.1016/j.autcon.2024.105559

[10] Liu, M.L., Wang, X., Zhong, Z.H. and Xiao, Y.S. (2026) 3-D DIC Camera Self-Motion Compensation Based on Automatic Selection of Reference Features. *Laser Technol-*

ogy, **50**, 99-107. (In Chinese)

[11] Zhang, Z. (2000) A Flexible New Technique for Camera Calibration. *IEEE Transactions on Pattern Analysis and Machine Intelligence*, **22**, 1330-1334. https://doi.org/10.1109/34.888718

[12] Conrady, A.E. (1919) Decentred Lens-Systems. *Monthly Notices of the Royal Astronomical Society*, **79**, 384-390. https://doi.org/10.1093/mnras/79.5.384

[13] Pan, B., Xie, H. and Wang, Z. (2010) Equivalence of Digital Image Correlation Criteria for Pattern Matching. *Applied Optics*, **49**, 5501-5509. https://doi.org/10.1364/ao.49.005501